

Breathable, Flexible, Transparent, Hydrophobic, and Biotic Sustainable Electrodes for Heating and Biopotential Signal Measurement Applications

Ijlal Haider, Milad Mosallaei, Kyriacos Yiannacou, Antti Vehkaoja, Setareh Zakeri, Veikko Sariola, and Vipul Sharma*

Pressure to reduce the global amount of e-waste has increased in recent years. The optimal use of natural resources is a demanding area especially due to the overabundance of the use of resources and challenges with after-life disposal. Herein, an easy method is developed to fabricate an improved version of leaf skeleton-based biodegradable, transparent, flexible, and hydrophobic electrodes. A fractal-like rubber leaf skeleton is used as the substrate, physical vapor deposited Au interlayer to promote adhesion, and uniform deposition of overlayer silver nanowires. The fabricated surfaces present a high level of electrical stability, optical transparency, hydrophobicity, and robust mechanical properties. The prepared electrodes demonstrate a comparable level of optical transmittance to the virgin leaf skeleton. The mechanical sturdiness of the electrodes is verified by 1k bending cycles. To demonstrate the functionality of these hybrid biotic conductive network (HBCN) electrodes, their performance is evaluated as flexible transparent heating elements and as biosignal measurement electrodes. The heater can reach a temperature of 140 °C with only 2.5 V in ≈ 5 s and Ag nanowire loading of $\approx 160 \mu\text{g cm}^{-2}$. Likewise, electrocardiogram (ECG) and electromyogram (EMG) signals are successfully obtained from the electrodes without using any electrode gel or other electrolytes.

1. Introduction

Flexible electronics is an interdisciplinary research area that combines a variety of research fields, such as chemistry, physics, material science, electronic and electrical engineering, mechanical engineering, computing science, and application-related fields such as biomedical engineering.^[1] The outcomes are compliant devices that can maintain mechanical integrity and electrical functionality while they are lightweight and conformable over uneven surfaces.^[2,3] Maintaining the mechanical and electrical integrity of the device during the deformation is the main challenge that needs to be addressed.^[2] In response to the challenges, the development of novel flexible materials and special mechanical designs are key remedies in designing the substrates and active components used in flexible electronics. There are commonly used flexible materials as substrate and conductive layers: either organic^[4,5] (e.g., small molecules, polymers) or inorganic^[6,7]


(e.g., metal nanowires, graphene, carbon nanotube). Likewise, different strategies in the structural design of stretchable systems are commonly used, such as in-plane/out-of-plane wavy structures, origami and kirigami structures as well as the island-bridge approach where rigid functional units are miniaturized and linked together by deformable interconnections.^[8–10] Among various kinds of applications, healthcare devices, including skin patches, smart clothing, and other devices that interface with the skin or other tissues are increasing their importance in remote patient monitoring and treatment.^[11]

Learning from nature provides a tremendous number of lessons for scientists to develop new materials and designs.^[12] Therefore, bioinspired materials with special functionalities have gained a lot of attention in engineering research. Scientists are inspired by the unique microstructures of these functional biological materials that can offer new features for various applications.^[13,14] Among the number of biostructure patterns, fractal-like structures are available in nature. Examples of fractal-like structures in nature are snowflakes and leaf skeletons. Fractal-like designs which offer high surface area, improved stability, and efficient transport of ions in the materials have been

I. Haider, M. Mosallaei, K. Yiannacou, A. Vehkaoja, V. Sariola, V. Sharma
Faculty of Medicine and Health Technology
Tampere University
Korkeakoulunkatu 3, 33720 Tampere, Finland
E-mail: vipul.sharma@tuni.fi

M. Mosallaei
Materials Processing and Circular Solutions
VTT Technical Research Centre of Finland
Visiokatu 4, 33101 Tampere, Finland

S. Zakeri
Materials Science and Environmental Engineering
Faculty of Engineering and Natural Sciences
Tampere University (TAU)
Korkeakoulunkatu 6, 33720 Tampere, Finland

 The ORCID identification number(s) for the author(s) of this article can be found under <https://doi.org/10.1002/adem.202201172>.

© 2022 The Authors. Advanced Engineering Materials published by Wiley-VCH GmbH. This is an open access article under the terms of the Creative Commons Attribution License, which permits use, distribution and reproduction in any medium, provided the original work is properly cited.

DOI: 10.1002/adem.202201172

reported.^[15] In the field of flexible electronics, one can take advantage of fractal-like designs as they present a higher surface area-to-volume ratio compared with conventional flat surfaces.^[16] Likewise, fractal designs can provide an efficient collection and transfer of electrical and thermal energy, and they have been applied in different applications such as photovoltaic, sensors, antennas, etc.^[17–19] Fractal-like patterns consist of a series of self-repeating patterns on different scales. More precisely, every part in a fractal pattern is very similar to the whole system.^[20] In such a design, the fractal pattern increases the surface coverage of the device by growing the orders of the fractal bridges.^[21] In a recent study, James et. al showed that the 3D fractal-like pattern can maximize the overall surface coverage, achieve a uniform current density as well as minimize the overall resistance for application in dye-sensitized solar cells (DSSC).^[15]

Several applications, e.g., in wearable electronics and biomedical engineering domains, require a high level of optical transparency.^[22] Therefore, transparent conductive layers with high electrical conductivity are highly demanded. Moreover, the higher surface coverage in self-repeated designs allows for increasing the loading number of functional materials (e.g., Ag nanowires) and contains numerous charge-transfer paths compared to flat surfaces, which maximizes the electrical conductivity accordingly. The fractal design can be replicated artificially. However, the process consists of a couple of steps such as lithography-based approaches^[20] and requires precise modeling. One can also take an advantage of utilizing natural designs directly by using natural and overabundance leaves that contain fractal structures in their skeleton.

In our previous work, we developed a biocompatible, flexible, and transparent electrode for heaters by using a fractal-like leaf skeleton and silver nanowires where we used a drop-cast method for the deposition of nanowires on the leaf skeletons.^[16] The fractal-like structure of the leaf skeleton tends to increase the surface area to volume ratio which improves the electrical conductivity of the electrode even during the bending. Herein, we propose an improved design of the leaf-skeleton-based electrode which is more electrically stable and shows hydrophobic behavior. Before the deposition of Ag nanowires, a thin layer of gold was coated on the surface in a sputtering process. The additional hydrophilicity provided by the Au layer along with the attractive forces originated by the metal–metal interactions would promote the consistent spreading of Ag nanowire solution on the leaf. Moreover, the adhesion of the overlayer Ag nanowires to the leaf was improved which resulted in a more uniform electrical conductivity along the electrode and hence the heat uniformity. Likewise, the electrode was able to maintain its conductivity during the bending for 1000 cycles. The electrodes developed in this work were demonstrated as a flexible heating element as well as a dry biopotential electrode.

2. Results and Discussion

For the preparation of the flexible electrodes, we used the leaf skeleton of the rubber tree which has a fractal-like structure composed of lignin and other biomaterials as the base substrate. The surface properties such as wettability influence the fabrication processes in multilayer devices. The same also applies in the case

of nanowire deposition onto the surfaces for device fabrication. Hence, a thin Au layer was physical vapor deposited by sputtering on the surface that allows improvement in wetting of the surface due to potential oxide formation as reported in ref. [23]. A simple drop-cast approach was used to deposit the Ag nanowire in water onto the leaf skeletons. The attractive forces originated due to the metal–metal interaction also allow Ag nanowires to attach uniformly to the surface. In addition to a thin Au layer, the presence of the microstructures and porous architecture soaks the water and allows the nanowires to form a network across the skeleton surfaces. The final conductive surfaces (HBCN) with the Au layer and the Ag nanowires with Ag concentration of $\approx 160 \mu\text{g cm}^{-2}$ displayed a uniform sheet resistance of $\approx 5 \pm 1 \Omega \text{ Sq}^{-1}$. The detailed fabrication procedure is discussed in the materials and methods section and the corresponding fabrication schematic is shown in **Figure 1**.

The morphology of the surfaces was investigated with scanning electron microscopy (SEM). **Figure 1b** shows the scanning electron micrograph of HBCN electrode based on *Hevea brasiliensis* (rubber tree). A network of Ag nanowires of length $\approx 50 \text{ nm}$ is visible and is conformally adhered across the Au-coated skeleton surface. Web-like distribution of the nanowire is not observed, which is common during the deposition of Ag nanowires on normal surfaces and covers the whole surface underneath.^[24] **Figure S1**, Supporting Information, shows the structure of the vascular bundles along with the interconnected fibers of the *H. brasiliensis* where the fiber interconnection gap is calculated to be in the range of $\approx 50\text{--}200 \mu\text{m}$ and short cell blocks in the range of $\approx 5\text{--}15 \mu\text{m}$ that are known to provide better flexibility to the skeletal structures as reported elsewhere.^[16] **Figure S2**, Supporting Information, shows the SEM image of Ag nanowire-coated skeleton surfaces without Au coating. From the SEM image, it can be seen that the Ag nanowires are present on the skeleton surface, but not attached very conformally as compared to HBCN where the Au layer is present beneath (refer **Figure 1b**).

To confirm the even distribution of the Au layer, Ag nanowires, and hydrophobic layer on the skeleton surface, the energy-dispersive X-ray spectroscopy (EDS) measurements were done. The EDS mapping data corresponding to the SEM images are shown in **Figure 2** which confirms the presence of an evenly spread Au layer, Ag nanowires, and a hydrophobic layer spread across the surface of the leaf skeleton. The element Si and a trace amount of Na are present in the commercial organic hydrophobic solution. The elements C, N, O, and K are also evident, which are the main constituents of the leaf skeleton.

To further investigate the effect of different coatings used in this study on the crystalline phases of the *H. brasiliensis* skeleton surface, X-ray diffraction (XRD) characterization was conducted. **Figure 2c** shows the X-ray diffractogram of *H. brasiliensis* skeleton surface coated with Ag nanowire, Au film, Au film–Ag nanowire, and Au film–Ag nanowire–hydrophobic layer. As can be seen from the black, red, and blue curves, the Ag nanowire (04-014-0266 XRD card), Au film (04-003-5615 XRD card), and Au film–Ag nanowire coatings (04-002-1174 XRD card) have overlapping X-ray diffractograms, and their main characteristic peaks are located at 38° , 44° , 64° , 77° , 82° , and 98° . This is due to the similar lattice constants of Ag and Au which also causes their alloy Ag nanowire on Au films to have similar

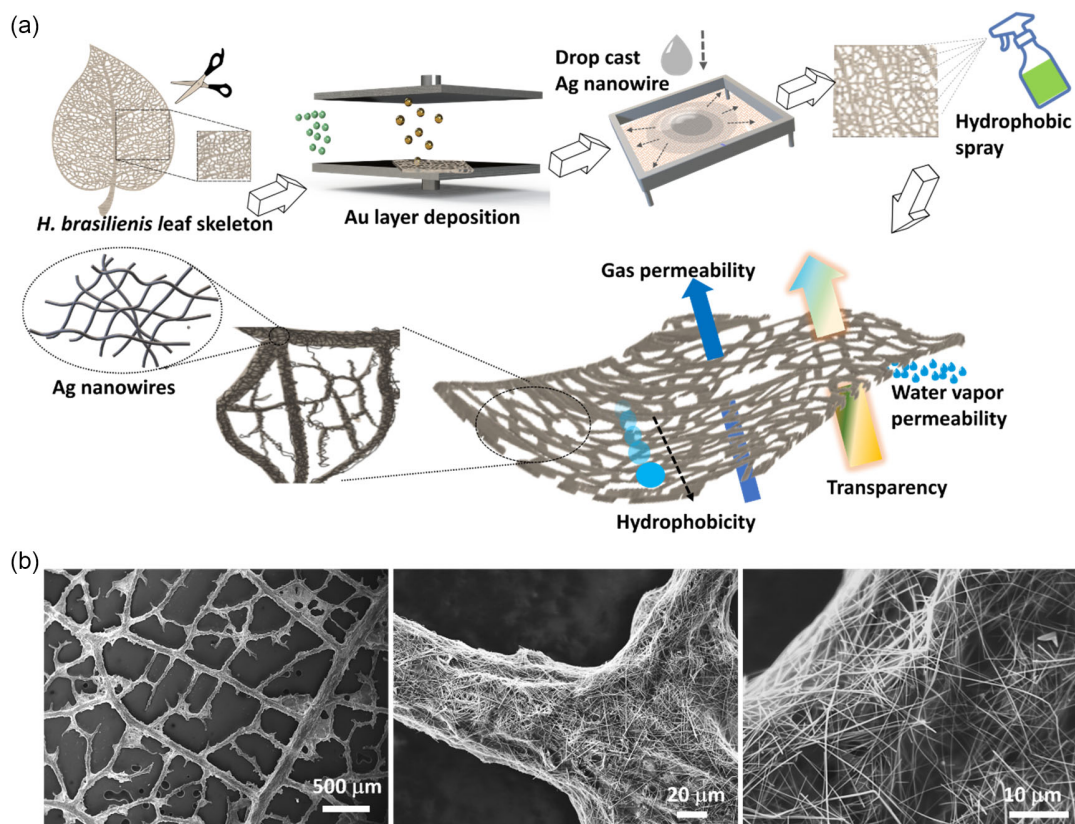


Figure 1. a) Schematic of the fabrication procedure and b) scanning electron micrographs of hybrid biotic electrodes in different resolutions.

XRD characteristic peaks. In addition, the data in the graph also confirmed that the presence of hydrophilic film did not change the metallic characteristics of the surfaces and there is no presence of any impurity that may hinder the performance of conducting surfaces as the corresponding curve is matching with the blue curve.

Stability and robustness are important parameters for electrodes that are used in flexible devices. In this regard, the resistance variation of the HBCN is investigated, as it experiences bending, cyclic bending, and exposure to a variety of electrolytes having different pH ranges. In our previous report, we already proved that the leaf skeleton is very flexible and maintains electrical conductivity even when bent.^[16] As this report addresses the improved design of leaf-based flexible electrodes with Au film underneath Ag nanowires and a hydrophobic film over it, it is important to test the flexibility of the new design. To check this, the HBCN was clamped and bent using a mechanical tester. For the small bending, the sheet resistance values did not change. As increasing bending strain was applied to the HBCN, the resistance values between the two clamped edges change only slightly but returned to their original value when returned to their initial position as shown in **Figure 3a**. The bending was continued up to 1000 cycles as shown in **Figure 3a**. After being bent for 1000 cycles at the maximum curvature of 500 m^{-1} , the HBCN displays only a slight change in the resistance values on repeated bending along with a decent recovery when returned to the original position each time as shown in **Figure 3a**.

To evaluate the stability of the HBCN, adhesion measurements were conducted using scotch tape. A tape was applied to the surface, pressed with the finger, and then peeled off after 5 s. **Figure 3b** displays the I - V curve of the HBCN after multiple tape cycle tests. As shown in **Figure 3b**, the HBCN maintained very good conductivity even after five cycles of tape test. The Au film allows additional electrical stability and allows better adhesion to the Ag nanowires. **Figure S3**, Supporting Information, shows the I - V curves of the control electrodes with Ag nanowires and Au film–Ag nanowires after the cyclic peel tests where the presence of Au film underneath clearly displays the better performance. In addition, the hydrophobicity is also maintained after five cycles as shown in **Figure S4**, Supporting Information. This is because of 3D surface architecture of the fractals only allows a little part to meet the tape and provide shielding to the rest of the parts. In addition, this also proves that the hydrophobic layer adheres nicely to the surface.

Transmittance measurements were performed to understand the relative transparency values of the rubber leaf skeleton. For this aim, the transparency of the leaf skeleton without any coating was compared to the ones coated with Au film, Au film–Ag nanowire, and HBCN in regions ranging from visible to near-infrared (300–800 nm). **Figure 3c** shows that different coating layers have negligible effects on the transparency of the whole electrodes which ensures that the transparency in the final conductive surfaces is maintained.

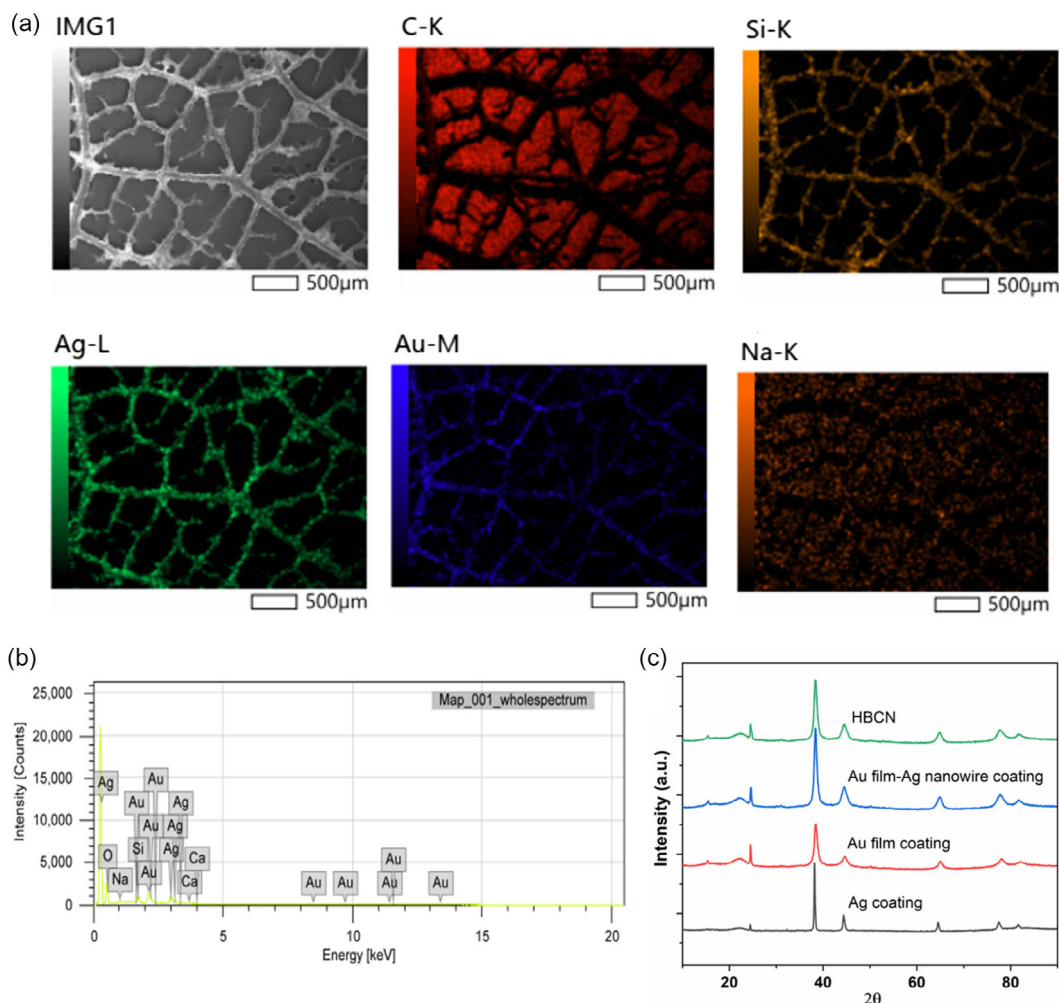


Figure 2. a) EDS mapping and b) EDS spectra of the hybrid biotic electrodes showing the uniform coverage of Ag throughout the surface. c) XRD spectra of the *H. brasiliensis* skeleton surface with Ag nanowire coating, Au coating, Au–Ag nanowire coating, and HBCN surfaces.

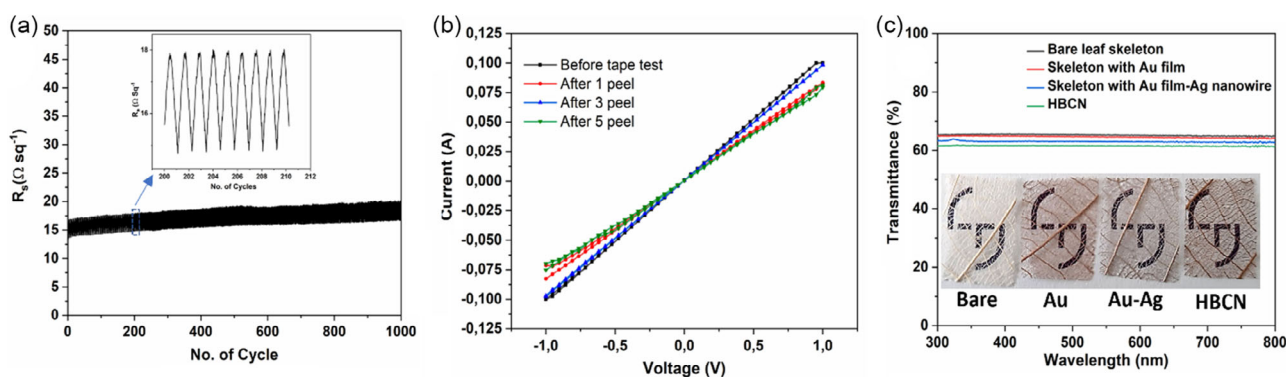


Figure 3. a) Normalized resistance variation when the HBCN is subject to cyclic bending. b) I – V curves of the time of tape test for the HBCN. c) Optical transmittances of HBCN along with the control samples. Inset shows the camera images displaying the corresponding transparency.

As mentioned, it is desired that the conductive leaf skeletons can be used in harsh environments such as humid, acidic, and alkaline conditions and should have anticorrosion properties. Also, Ag nanowire-based electrodes are prone to oxide formation

on the surface; hence their shelf life is affected. The hydrophobic layer used in this study attaches very nicely and conformally to the Ag surface, hence displaying good hydrophobic performance. The introduction of the hydrophobic layer can effectively prevent

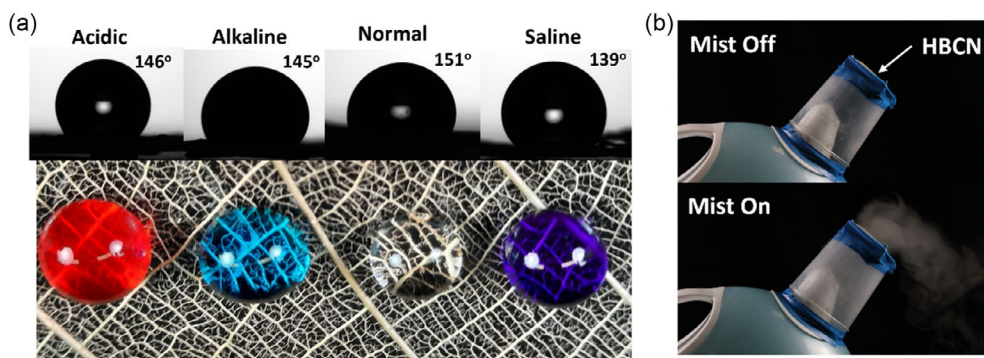


Figure 4. a) Contact angles of the HBCN with alkaline, normal, acidic, and saline solutions. Camera images show the corresponding droplets maintaining the spherical shape over the HBCN surface. b) The breathability of the HBCN where the surface allows the cool mist generated by the humidifier to pass through it.

the aqueous solution penetration into the Ag nanowire or leaf skeleton. The pure water droplets and the droplets with the acidic, salt, and alkaline solutions displayed high contact angles on the HBCN surface. The water contact angles are above $\approx 140^\circ$ as displayed in **Figure 4a**. The water droplets in all the solutions display very good spherical shapes on the surface of the HBCN. To check the stability of the electrode, the surface was also put in acidic, alkaline, and salt solutions. Due to the hydrophobicity and small amount of air trapped inside the skeleton, the surface floated on the surface using solutions that can be seen in **Figure S5**, Supporting Information. The surfaces displayed almost the same contact angles even after floating in the harsh solutions for 2 h and the surfaces remained hydrophobic. There was almost no change in the sheet resistance of the surface after the tests confirming the high stability of the biotic electrode. In addition, the self-cleaning behavior of the HBCN was also demonstrated which is shown in **Video SV1**, Supporting Information. A small amount of soil was put on the surface of HBCN which was removed using the water droplets, confirming the self-cleaning behavior of the surface.

Breathability is very important for conducting surfaces that are applicable in healthcare and other applications. It was not possible to conduct the gravimetric (dish) method^[25] to determine the water vapor permeability tests due to the micromesh architecture of the surface. However, to prove the water vapor transmission through the surface, we placed the surface in front of a commercial humidifier generating a fine cool mist. As shown in **Figure 4b** and **Video SV2**, Supporting Information, the vapors are seen passing through the biotic surface, confirming the breathability of the surface. To check the influence of humidity on the conductivity of the surface, the electrical conductivity was checked after the exposure of the surface to the cool mist for 60 min. It is noteworthy to mention that humidity seems to have little influence on the electrical conductivity of the surface. Even at very high humidity of $>85\%$ and prolonged exposure, the resistance only has a slight increase of $\approx 3\%$, which is acceptable. These results demonstrate the excellent stability of the electrical conductivity of the biotic conducting surfaces in a moist environment.

The Joule heating characteristics of the bioinspired bimetallic heater are studied. For performance comparison,

the concentration of the Ag nanowire in each electrode surface was $\approx 160 \mu\text{g cm}^{-2}$. We expected that a thin layer of Au beneath the Ag nanowire provides not only the uniform deposition of the Ag nanowires but also uniform heating across the surface. To check the heating to the surface, a continuous DC voltage (1.5 V) was applied between the two edges of the surfaces, and the infrared image was recorded as shown in **Figure 5a**. The leaf skeleton surface with just the Ag nanowire showed uniform heating across the surface, but there was a significant area where the heat distribution was uneven. The heating distribution was much more even in the surfaces with a thin layer of Au beneath the Ag nanowires (**Figure 5b**). The heating was also uniform in the HBCN as shown in **Figure 5b** and the presence of the hydrophobic layer did not have any significant effect on the heat distribution across the surface.

To check the response time, steadiness, and reliability of the surfaces as heaters, time-dependent temperature profiles were recorded. A constant DC voltage was applied to the connections made to the surface as shown in **Figure 5a**. **Figure 5d–f** displays the time-dependent temperature profiles of different heater surfaces. For each heater, the temperature was recorded at a range of voltages starting from 0.5 to 2.5 V. For the comparison, 2.5 V was set as the maximum voltage. In all the skeleton-based heaters, the temperature increased rapidly and reached a steady operating state within ≈ 10 s which is expected due to the fractal-like design that allows the rapid heating and cooling of the surface, owing to the high surface-to-volume ratio. However, there was a significant difference in the heating rates and maximum temperatures among the different biotic surfaces. The leaf skeleton surface with only Ag nanowires displayed a heating rate of $\approx 8^\circ\text{C s}^{-1}$ and an average maximum temperature of $\approx 105^\circ\text{C}$ at 2.5 V. In the case of the surface with Au film–Ag nanowire, the heating rate was $\approx 17^\circ\text{C s}^{-1}$ along with the average maximum temperatures exceeding $>150^\circ\text{C}$ at 2.5 V. The saturation temperature was achieved at this voltage which is evidenced by the flat line. The heater failed above this voltage due to the excessive temperatures that lead to the burning of the leaf skeleton support which can be seen in **Figure 5e**. The heating can be controlled by optimizing the amount of Ag nanowire on the surface as reported elsewhere.^[26] In the case HBCN, the heating rate was 12°C s^{-1} , and the average maximum steady-state

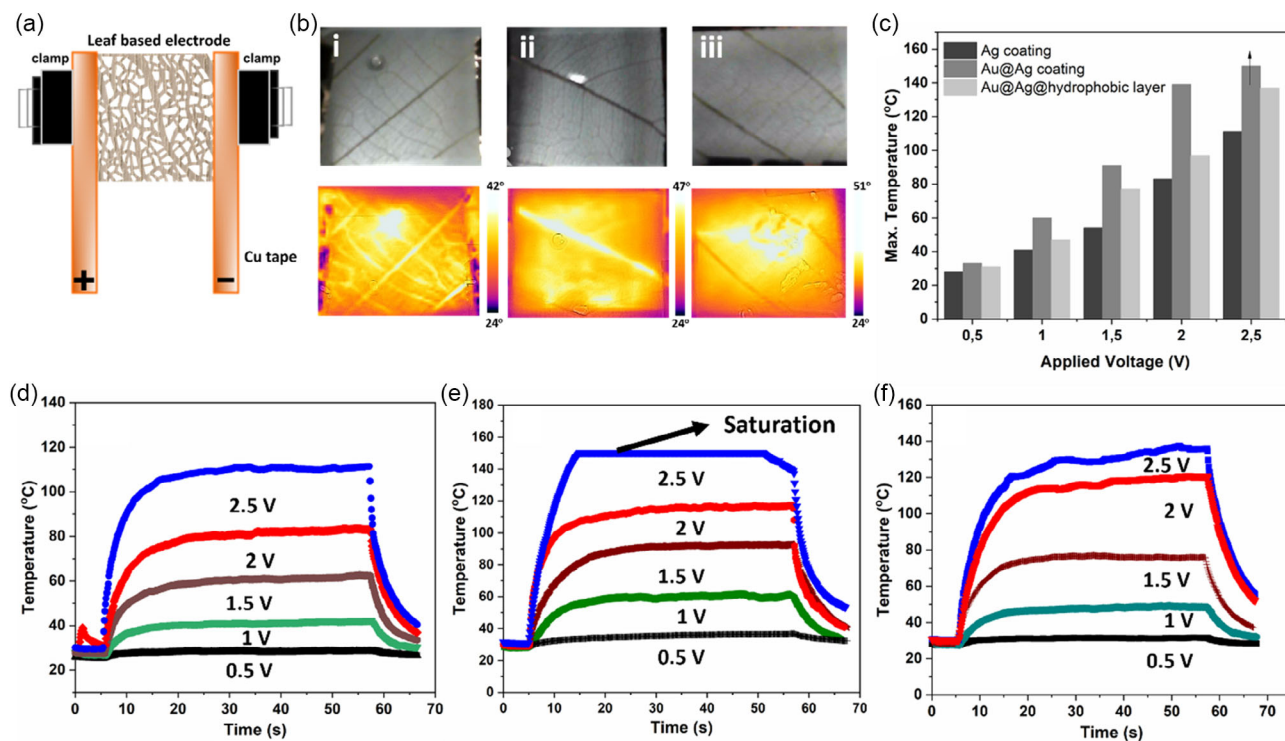


Figure 5. a) Thermal characterization of the electrodes with various coatings. b) Infrared camera images of the electrode with (i) only Ag nanowire only, (ii) Au film–Ag nanowire, and (iii) HBCN. c) Transient temperature evolution of the different electrodes as stepwise voltage rises from 0.5 to 2.5 V. Time-dependent surface temperatures of biotic electrodes at different voltages: d) skeleton with only Ag nanowire, e) with Au film–Ag nanowire, and f) HBCN. Ag nanowire loading in all the surfaces is $\approx 160 \mu\text{g cm}^{-2}$.

temperature of $\approx 130 \text{ }^\circ\text{C}$ at 2.5 V. A slight dip in the heating rate could be attributed to the hydrophobic layer that may limit the heat radiating out of the surface. From the experiments, it is clear that the presence of a thin Au layer beneath Ag nanowires helps in improving the efficiency of the electrodes when used as a heater. It is also noteworthy to mention that the presence of the hydrophobic layer does not significantly hinder the performance of the electrode as a heater.

The electromyogram (EMG) signal can be used in many applications, such as the diagnosis of muscle nerve discoordination, muscle fatigue monitoring, etc., while the electrocardiogram (ECG) signal provides important information about the human heart and its physiological function. When the electrodes for these applications are integrated into the flexible devices, it is difficult to obtain the signals because soft skin-like, electrically conducting, and biocompatible materials must be integrated with electrical circuits. Hence, dry electrodes are being developed for these purposes.^[27] However, most dry electrodes are fabricated on rigid substrates, which do not possess adequate flexibility and conformal attachment to human skin. Novel flexible/stretchable substrates are a topic of research in the state-of-the-art literature for dry electrodes in pursuit of wearable biopotential electrodes.^[27] The HBCN was applied to fabricate the dry electrodes for EMG and ECG as well. An additional thin layer of Au was added to the top of HBCN to make it suitable for biopotential measurements. Figure 5 shows 60 and 5 s excerpts of the recorded EMG and ECG signals without any signal

preprocessing i.e., with 0.05–150 Hz bandwidth. By visual observation, the electrode with top Au finishing provides a signal with noticeably less baseline noise. This is visible, especially when comparing the ECG signals. Both surface structures can however provide high-quality biopotential signals without any skin preparation facilitating their utility in long-term use. The quality of the signals from the biotic electrodes was compared to the commercially available dry electrodes (Ag/AgCl) as shown in Figure S6, Supporting Information. From Figure 6 and S6, Supporting Information, it is clear that the EMG and ECG data obtained from the biotic electrodes are at par with the commercially available electrodes.

From the results, it is clear that the electrodes based on the Au film and Ag nanowires displayed better electrical performance as an electrode and as heater surfaces as well. In addition, the surfaces were mechanically stable as well. There are a few reasons for this increase in performance. The first reason is the uniform distribution of the Ag nanowires onto the Au substrate. Due to the presence of a thin Au layer, Ag nanowires dispersed in the water uniformly spread across the fractal surfaces, and a slight increase in hydrophilicity and porous architecture of the fractals in water helps them to adhere properly. It has been reported in the literature that Ag gets coated onto the Au properly and it is known to make a very good metallization layer. Ag gets adhered to the surface of Au very nicely due to the work function (Φ) difference which is one of the reasons that smooth core–shell structures are feasible in the case of Au@Ag.^[28] It is also

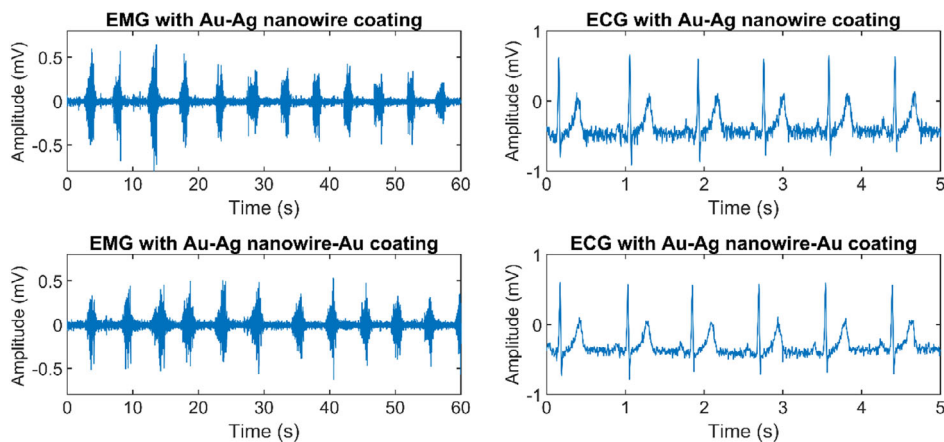


Figure 6. Examples of EMG (left panels) and ECG (right panels) signals recorded Au film–Ag nanowire-coated (top) and Au film–Ag nanowire–Au-coated (bottom) electrodes.

reported that the uniform Au and Ag contacts lead to higher carrier transport efficiency, which, in turn, leads to better electrical performance^[29] The Ag and Au junction joints also increase the shear tolerance of the surface and maintain the electrical contacts better than the monometallic surfaces. As lignin is the main constituent of the leaf skeletons along with the organic hydrophobic spray, the surfaces can be considered as biodegradable. The biodegradation of the leaf skeletons has been demonstrated in our previous studies.^[30]

The optical, electromechanical, and thermal performance of the HBCN shows an improvement in performance as compared to the previously reported fractal-based systems. More precisely, the HBCN provides good flexibility as demonstrated in a large number of bending–relaxing cycles while the leaf maintains its mechanical integrity. In addition, the interlayer Au layer promotes the adhesion of Ag nanowires to the base leaf which synergistically improves the performance of the electrode. The high surface area of the fractal-like leaf skeleton compared to the flat surfaces allows higher loading of the conductive materials which directly improves the electrical and thermal performance of the device without sacrificing the optical transparency of the electrode.

3. Conclusions

In conclusion, we fabricated biodegradable, flexible, transparent, and hydrophobic conducting electrodes using rubber tree (*H. brasiliensis*) fractal-like leaf skeletons, Au-based adhesion promotion layer, Ag nanowires dispersed in water as a conductive material, and a commercial organic hydrophobic solution. These surfaces were applied as heaters and very good performances were observed. An additional layer of Au on top of the HBCN enables it to be used as electrodes in the biosignal measurement systems. The fabrication process, microstructures, transparency, thermal, mechanical, and biosignal properties of the electrodes were investigated in detail. The Ag nanowires are conformally and evenly attached to the fractal-like structures due to the sputtered Au adhesion promotion layer. Indeed, the

presence of an Au layer improves the adhesion and uniform distribution of the Ag nanowire on the surface. More than the high surface-to-volume ratio of the base leaf material which allows higher loading of functional substances, the uniform distribution of the Ag nanowires due to the Au layer, the heat uniformity, and the performance of the HBCN when used as the heater is increased once the device is powered. Finally, these electrodes were able to measure the biosignals from humans in a convenient way where they did not leave any effect on the skin. Majority of the materials used in the fabrication of these electrodes are eco-friendly, easily accessible, available in abundance, and easy to fabricate compared to the other transparent electrodes that require complex, expensive, and energy exhaustive fabrication processes.

4. Experimental Section

Materials: For the fabrication of the leaf skeleton electrode, leaf skeletons of *H. brasiliensis* were supplied by “Leaf Vein Crafts,” Toronto, Canada. Ag nanowires for the fabrication of conducting surfaces were purchased from Sigma-Aldrich, Finland. All the chemicals were used as received. Copper tape with conductive adhesive manufactured by 3M was used for making the electrical contacts.

Fabrication of the Electrode: In the first step, the leaf skeletons were cut in the dimensions $\approx 2\text{ cm} \times 2\text{ cm}$ and mounted onto a plastic frame with the help of tape. A thin layer of gold ($\approx 5\text{ nm}$) was sputtered on both sides of the leaves before Ag nanowire deposition. In the next step, small droplets of Ag nanowires (in water) were placed onto the leaf skeletons and spread like a paintbrush. Then the skeletons were transferred to the oven and dried at $\approx 100\text{ }^\circ\text{C}$ for 10 min. This step was repeated multiple times so that the final Ag nanowire concentration loaded was ($\approx 160\text{ }\mu\text{g cm}^{-2}$). Note that the concentration here is the concentration of the total Ag element and is calculated from the stock solution of Ag nanowires (5 mg mL^{-1}). After drying, copper tape (3M) was applied at the edges of the surfaces to make conductive contacts. To make the surface water repellent, leaves were sprayed with a fluorocarbons-free organic hydrophobic solution (OrganoTex Spray-On). The copper tapes were pressed with paper clips to keep the contact uniform. The final electrodes based on Hybrid Biotic Conductive Networks are called in this paper as HBCN for brevity.

Characterization: High-resolution surface structure characterization was performed using an SEM (Jeol IT-500) operating at 5–15 kV. The infrared images were captured using the FLIR One Pro infrared camera. The temperature at the surface was verified using a thermocouple. The sheet resistance of the surfaces was measured using the four-probe method using an LCR meter (Keysight Technologies E4980A Precision LCR Meter). The measurement was done by just simply connecting the probes of the LCR meter on our electrodes and the sheet resistance values were recorded. Image J software with the Fraclac plugin was used to analyze the surface coverage and fractal dimensions. Transmittance spectra were recorded using Cary 60 UV–vis Spectrophotometer (Agilent Technologies). XRD analysis was performed to identify the crystalline phases using a Panalytical Empyrean multipurpose X-ray diffractometer (PANalytical B. V., The Netherlands) equipped with a Cu K α radiation source (powered at 45 kV and 40 mA). The scattered intensities as a function of the scattering angle 2θ (10°–100°) were measured by a PIXcel 3D detector. The Panalytical HighScore Plus software (version 3.0.5) was used for phase identification, together with the International Centre for Diffraction Data database PDF-4+ (Database version 4.1065).

EMG and ECG Measurements: The performance of the proposed leaf skeleton electrodes for the measurement of ECG and EMG was evaluated with a bipolar electrode setup utilizing Biopac MP36 measurement equipment. In both measurements, the electrodes with approximately 5 cm² area were applied on the skin using mechanical compression force of approximately 1 N provided with regular ECG clamp electrodes. The electrodes were applied to the skin without any preparation to mimic an actual use scenario. No electrode gel or other electrolyte was used in the measurements. The measurement was started after less than 1 min of settling time. The electrodes were placed on the palmar side of the forearm. In the case of the ECG measurements, the electrodes were placed on both arms 5 cm proximal from the wrist. The subject was staying still during the 5 min recording. In the case of the EMG measurements, the electrodes were placed on the palmar side of the right forearm, 20 cm apart from each other. The subject was squeezing the palm to fist sequentially to activate the forearm muscles. 2 kHz sampling rate and 0.05–150 Hz passband were used in both ECG and EMG measurements.

Supporting Information

Supporting Information is available from the Wiley Online Library or from the author.

Acknowledgements

This work was supported by the Academy of Finland (grants: #331368, #299087, #292477, and #326461) and KONE foundation. All authors are grateful for the support from the Tampere Microscopy Center for the characterization of the surfaces.

Conflict of Interest

The authors declare no conflict of interest.

Data Availability Statement

The data that support the findings of this study are available from the corresponding author upon reasonable request.

Keywords

Ag nanowires, bioinspiration, electrocardiography, electromyography, flexible electronics

Received: August 15, 2022

Revised: October 18, 2022

Published online:

- [1] K. Liu, Y. Bian, J. Kuang, Q. Li, Y. Liu, W. Shi, Z. Zhao, X. Huang, Z. Zhu, Y. Guo, Y. Liu, *Giant* **2021**, 7, 100060.
- [2] K. D. Harris, A. L. Elias, H.-J. Chung, *J. Mater. Sci.* **2016**, 51, 2771.
- [3] D. Corzo, G. Tostado-Blázquez, D. Baran, *Front. Electron.* **2020**, 1, 2.
- [4] J. S. Noh, *Polymers* **2016**, 8, 123.
- [5] V. Zardetto, T. M. Brown, A. Reale, A. Di Carlo, *J. Polym. Sci., Part B: Polym. Phys.* **2011**, 49, 638.
- [6] M. U. Ocheje, B. P. Charron, A. Nyayachavadi, S. Rondeau-Gagné, *Flex. Print. Electron.* **2017**, 2, 043002.
- [7] K. Sugauma, *Springer Briefs in Electrical and Computer Engineering Introduction to Printed Electronics*, Springer, New York **2014**.
- [8] W. Wu, *Sci. Technol. Adv. Mater.* **2019**, 20, 187.
- [9] X. Yu, B. K. Mahajan, W. Shou, H. Pan, *Micromachines* **2016**, 8, 7.
- [10] Y. Zhao, J. Guo, *InfoMat* **2020**, 2, 866.
- [11] D. Dias, J. P. S. Cunha, *Sensors* **2018**, 18, 2414.
- [12] G. M. Whitesides, *Interface Focus* **2015**, 5, 20150031.
- [13] W. Li, Y. Pei, C. Zhang, A. G. P. Kottapalli, *Nano Energy* **2021**, 84, 105865.
- [14] S. Abedanzadeh, M. Nourisefat, Z. Moosavi-Movahedi, *Rationality and Scientific Lifestyle for Health*, Springer, Cham **2021**, pp. 9–29.
- [15] S. James, R. Contractor, *Sci. Rep.* **2018**, 8, 1.
- [16] V. Sharma, K. Jääskö, K. Yiannacou, A. Koivikko, V. Lampinen, V. Sariola, *Adv. Eng. Mater.* **2022**, 24, 2101625.
- [17] G. K. Soni, S. Gour, A. Sharma, *Emerging Trends in Data Driven Computing and Communications*, Springer, Singapore **2021**, pp. 203–211.
- [18] J. A. Fan, W. H. Yeo, Y. Su, Y. Hattori, W. Lee, S. Y. Jung, Y. Zhang, Z. Liu, H. Cheng, L. Falgout, M. Bajema, T. Coleman, D. Gregoire, R. J. Larsen, Y. Huang, J. A. Rogers, *Nat. Commun.* **2014**, 5, 3266.
- [19] Y. Liu, K. He, G. Chen, W. R. Leow, X. Chen, *Chem. Rev.* **2017**, 117, 12893.
- [20] E. J. W. Berenschot, H. V. Jansen, N. R. Tas, *J. Micromech. Microeng.* **2013**, 23, 055024.
- [21] Z. Wang, L. Sun, Y. Ni, L. Liu, W. Xu, *Front. Nanotechnol.* **2021**, 3, 1.
- [22] L. F. Gerlein, J. A. Benavides-Guerrero, S. G. Cloutier, *Sci. Rep.* **2021**, 11, 24156.
- [23] M. L. White, *J. Phys. Chem.* **1964**, 68, 3083.
- [24] L. Zhang, T. Song, L. Shi, N. Wen, Z. Wu, C. Sun, D. Jiang, Z. Guo, *J. Nanostruct. Chem.* **2021**, 11, 323.
- [25] R. P. Brown, *Physical Testing of Rubber*, 3rd ed., Chapman & Hall, London **1996**, 92–97.
- [26] V. Sharma, A. Koivikko, K. Yiannacou, K. Lahtonen, V. Sariola, *npj Flex. Electron.* **2020**, 4, 1.
- [27] P. Fayyaz Shahandashti, H. Pourkheyrollah, A. Jahanshahi, H. Ghafoorifard, *Sens. Actuators, A* **2019**, 295, 678.
- [28] V. Sharma, N. Sinha, S. Dutt, M. Chawla, P. F. Siril, *J. Colloid Interface Sci.* **2016**, 463, 180.
- [29] Y. Kuo, *ECS Trans.* **2015**, 69, 23.
- [30] A. Koivikko, V. Lampinen, K. Yiannacou, V. Sharma, V. Sariola, *IEEE Sens. J.* **2022**, 22, 11241.